# A Switched-Mode Multichannel Neural Stimulator with a Minimum Number of External Components

Marijn N. van Dongen and Wouter A. Serdijn

Biomedical Electronics Group, Delft University of Technology, The Netherlands

Email: M.N.vanDongen@tudelft.nl

*Abstract*—This work proposes a system design for neural stimulators. It eliminates the need for a DC-DC converter which is normally used to increase the battery voltage. Instead it combines the DC-DC converter and stimulator output stage into a single system block. The number of external components needed for the system is reduced to a single inductor only.

The system offers high power efficiency operation (theoretical power efficiency of 100% and a simulated efficiency of around 60% over the full output range) by employing switched-mode operation. Furthermore the output has a current source character, making charge balanced stimulation relatively easy to implement.

Finally it is also possible to stimulate multiple channels independently with this system. An example design is presented that can stimulate two channels with a maximum output voltage of $10\,\text{V}$, while being powered from a $3.5\,\text{V}$ battery.

## I. Introduction

Implantable neurostimulators are generally battery operated. Batteries suitable for medical applications usually have an operating voltage between $3\,\text{V}$ and $4\,\text{V}$. This means that the input energy source of a neurostimulator can be assumed to be a *voltage source* with a value $V_{\text{in}}$ in that range.

The output quantity of a neurostimulator can be either a voltage or a current, though a minimum amount of current $I_{\text{r}}$ (Rheobase current) is required to make the electric field strong enough to achieve stimulation. That means that for a given electrode/tissue impedance $Z_e$, the minimum required output voltage is $V_{\text{stim}} = I_{\text{r}} Z_e$. The absolute values of $I_{\text{r}}$ and $Z_e$ heavily depend on the application, but in general $V_{\text{stim}} > V_{\text{in}}$.

For this reason many implantable neurostimulators adopt an architecture similar to the one depicted in Figure 1a. First a DC-DC converter is used to increase the supply voltage up to the maximum stimulation voltage that can be expected, $V_{\text{dd}}$. Subsequently a stimulator output stage is designed that uses $V_{\text{dd}}$ to stimulate the tissue. A few drawbacks of this scheme can be identified:

- The DC-DC converter is using an absolute minimum of 2 (bulky) external components: an inductor for voltage boosting and a capacitor for stabilizing the output voltage. External components are in general undesired: they are bulky, expensive and involve an additional reliability risk.
- Many of the designs for stimulator output stages use additional external components. Examples include capacitors used for charge cancellation or mid-rail reference buffering [1].
- When $V_{\text{dd}} > V_{\text{stim}}$ the DC-DC converter is generating a too high voltage, which will limit the power efficiency



(a) Most existing architectures use a $V_{\text{dd}} >> V_{\text{stim}}$



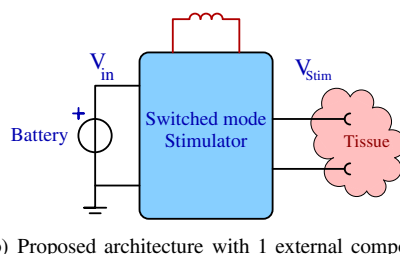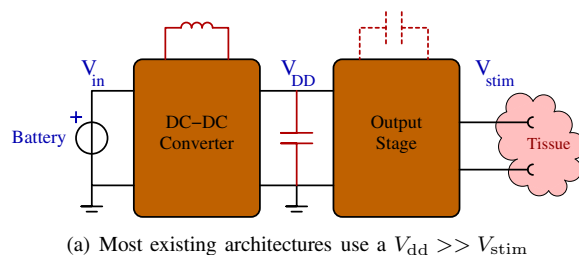(b) Proposed architecture with 1 external component

Fig. 1. Stimulator architectures with external components indicated in red

to $\eta = V_{\text{stim}}/V_{\text{dd}}$. Since energy efficiency is of crucial importance in the design of implantable stimulators, this is a major concern.

Several solutions have been proposed for the latter drawback relating to the power efficiency. It is possible to adapt $V_{\text{dd}}$ to the $V_{\text{stim}}$ needed by the stimulator (class G or H operation) [2], [3]. Recently another architecture was proposed using a switched mode output stage (class D operation) [1]. However, still a DC-DC converter is required that will first create a too high $V_{\text{dd}}$, which is down converted afterwards.

The solution proposed in this paper has been developed independently of [1] and offers a few additional advantages. It is possible to use one single inductor for both voltage conversion as well as signal handling, while still achieving energy efficient operation. It is even possible to use this single inductor to simultaneously stimulate multiple channels independently. The resulting system is depicted in Figure 1b.

## II. System design

The basic operation of the system is based upon class D operation because of the high power efficiency: a switched-mode circuit is used to directly stimulate the tissue. In Figure 2 this is illustrated for a switched converter circuit based on a Buck-boost-converter architecture. It is also possible to use

buck- or boost architectures, depending on the requirements for $V_{\text{stim}}$.

## A. Switching frequency and output capacitor

A capacitor needs to be placed in parallel with the output of the converter to filter out the switching transients (reduce the ripple in the output voltage). This capacitor needs to be chosen such that the cut-off frequency is lower than the switching frequency.

For an implantable stimulator it is not desired to include a big (and therefore external) capacitor at the output. However, when we look at the model of the tissue in Figure 2, it is seen that there actually is a capacitor available in the load of the system: the tissue itself.

The tissue is usually modeled in two parts: the capacitive electrode-tissue interface $C_{\text{if}}$ and the tissue itself. In almost all cases the tissue is assumed to be purely resistive ($R_{\text{tis}}$). However the tissue also has dynamic properties [4], which can be modeled using a capacitor $C_{\text{tis}}$.

On short time scales $C_{\text{tis}}$ will be dominant, because $C_{\text{if}} \gg C_{\text{tis}}$. That means that at these timescales the tissue itself already introduces the output capacitor. Therefore if the switching frequency is made high enough, the output capacitance can be omitted!

The time constant of tissue has been found to be in the order of $1\,\mu s$ [4]. Therefore it was chosen to operate the system at a switching frequency of $f = 2\,\text{MHz}$.

To generate for example a stimulation pulse with a pulse width of $100\,\mu s$ a total of 200 switching cycles is generated. This is shown in Figure 3 for a biphasic stimulation pulse. The tissue will filter the pulses and the resulting tissue voltage is shown: the high frequency components are removed in the electric field. This shows the high frequency stimulation can mimic the classic stimulation, but with a much higher efficiency and with only one external inductor.

In reality the tissue exhibits quite a lot of dispersion: the time constant is frequency dependent. This has been measured experimentally and is described in [5]. This influence of dispersion can be accounted for in simulations and will increase the ripple in the electric field (due to the decreasing time constant for higher frequencies). However, there will still be a DC component in the electric field.

## B. Safety

One of the key safety aspects of safe stimulation is charge cancellation. Therefore the direction of current needs to be inverted after a stimulation pulse. This is accomplished by introducing an H-bridge in the circuit as shown in Figure 2. The resulting biphasic stimulation waveform is shown in Figure 3.

To achieve actual charge cancellation various methods can be applied such as pulse insertion [6] or dynamic offset cancellation [7], [8]. For all these methods the circuit has the advantage that the output has a current source characteristic (because of the inductor). The amount of charge injected in a cycle is therefore easily controlled.
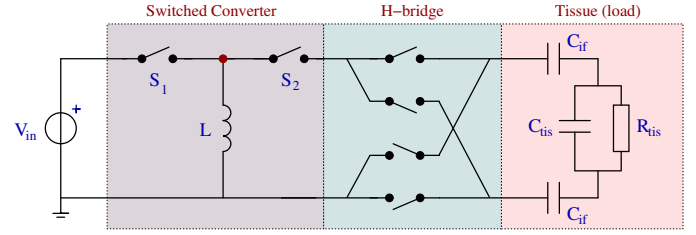


Fig. 2. System design of the proposed stimulator. The converter is depicted here in Buck-boost mode, although Boost and Buck modes are also possible

One aspect that is currently unknown is how the tissue will exactly react on the pulsed current stimulation. Although the electric field that is responsible for stimulation, is relatively constant the effect of the current pulses is not known. To test this a discrete component realization was fabricated, which will be discussed later.

## C. Multichannel operation

It is possible to stimulate multiple channels simultaneously and independently with one single inductor. The key in this is to operate the switched-mode circuit in discontinuous mode. If the duty cycle of the switching circuit is kept low, a full cycle (charging and discharging of the inductor) can be completed within 50% of a switching period. That means that in the remaining time it is possible to stimulate another channel with another intensity.

This is illustrated in Figure 3. During one switching cycle the inductor is first charged to about $22\,\text{mA}$ and is discharged through Channel 1. During the same switching cycle the inductor is subsequently charged to about $12\,\text{mA}$ and discharged through Channel 2. The resulting channel voltages are also plotted in the figure.

Note that adding an additional channel effectively doubles the switching frequency of the system. The number of channels that can be connected to one inductor is limited by how low the duty cycle can be set.

## III. SYSTEM LEVEL SIMULATIONS

The average output voltage $\hat{V}_{\text{out}}$ is easily found for a buck-boost converter. First the energy delivered by the source during charging of the inductor is considered:

$$E_{\text{source}} = \int_0^{\delta T} I(t)V_{\text{dd}}dt \approx \int_0^{\delta T} \frac{V_{\text{dd}}^2}{L}tdt = \frac{V_{\text{dd}}^2}{2L}(\delta T)^2 \quad (1)$$

Here $T$ is the period of the switching and $L$ is the inductance. Furthermore, the average energy consumed in the load is $E_{\text{load}} = T\hat{V}_{\text{out}}^2/R$, where $R$ is the tissue resistance and $\hat{V}_{\text{out}}$ is the average output voltage. By using that for an ideal system it holds $E_{\text{source}} = E_{\text{load}}$, it is found that:

$$\hat{V}_{\text{out,buckboost}} = \sqrt{\frac{V_{\text{dd}}^2\delta^2 TR}{2L}} \quad (2)$$

Note that this equation is independent of the capacitance (i.e. the time constant) of the tissue. For smaller time constants the ripple of the output voltage will be bigger, but the average
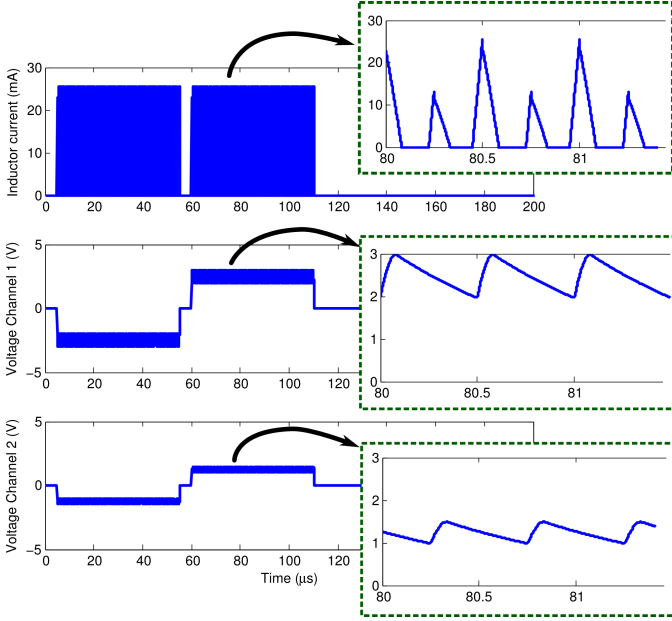
Fig. 3. The waveforms of the switched-mode stimulator in Buck-boost mode during a full stimulation cycle. Two channels are simultaneously stimulated independently using only one external inductor.



(a) PCB realization      (b) Tissue voltage

Fig. 4. Discrete component implementation and measurement results of the HF stimulator

output voltage will be constant. A similar relation can be found for boost and buck converters, although the equations are slightly more complicated:

$$\hat{V}_{\text{out,boost}} = \frac{V_{\text{dd}}\left(L + \sqrt{L\left(2RT\delta^2 + L\right)}\right)}{2L} \qquad (3)$$

$$\hat{V}_{\text{out,buck}} = \frac{-RV_{\text{in}}\delta\left(\delta T - \sqrt{\left(T^2\delta^2 - 8LT\right)/R}\right)}{4L} \qquad (4)$$
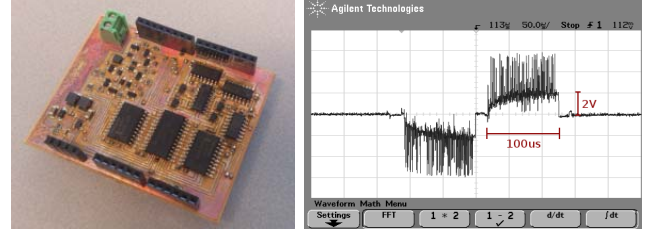
To find expressions for the transient waveforms numerical methods are applied. The system will be designed for use with micro-electrodes, meaning a high impedance. The maximum output current was assumed to be $100\,\mu\text{A}$ and the tissue was modeled with $R = 100\,\text{k}\Omega$, which means that $C = 10\,\text{pF}$, assuming a non dispersive medium with $\tau = 1\,\mu\text{s}$. The input voltage was assumed to be $V_{\text{in}} = 3.5\,\text{V}$.

The value of the inductor can be determined based on the ratio $\hat{I}_{\text{out}}/I_{\text{peak}}$ in which $I_{\text{peak}}$ is the peak current in the inductor and $\hat{I}_{\text{out}}$ is the average output current. If a maximum ratio is chosen, the minimum value of the inductor is determined by:

$$L > 2RT\left(\frac{\hat{I}_{\text{out}}}{I_{\text{peak}}}\right)^2 \qquad (5)$$

The rate at which the inductor can be charged and discharged to keep the system in discontinuous mode sets the maximum value of the inductor:

$$L < \min\left(RT_{\text{dis}}\frac{\hat{I}_{\text{out}}}{I_{\text{peak}}}, \frac{V_{\text{dd}}\delta_{\text{max}}T}{I_{\text{out,max}}}\frac{\hat{I}_{\text{out}}}{I_{\text{peak}}}\right) \qquad (6)$$

Where $T_{\text{dis}}$ is the maximum time allowed for the inductor to discharge. Based on these equations it was chosen to have $L = 70\,\mu\text{H}$.

The resulting waveforms are depicted in Figure 3 for an ideal (lossless) buck-boost setup. Channel 1 uses a duty cycle of 0.1, while channel 2 uses a duty cycle of 0.05.

### A. Losses

The losses in the system can be subdivided in two categories: resistive and capacitive losses. Resistive losses occur because of the limited on-resistance $R_{\text{ds,on}}$ of the switches. Resistive losses increase for increasing output levels due to the higher current peaks in the system.

The capacitive losses occur mainly due to the parasitic capacitance $C_{\text{par}}$ at the switching node (marked in red in Figure 2). Capacitive losses are dominant at low output levels, when relatively more of the energy is lost in charging and discharging the parasitic capacitor. Because of the relatively high switching frequency this circuit suffers more from capacitive losses.

It is now possible to select the optimum transistor dimensions for which the combination of $R_{\text{ds,on}}$ and $C_{\text{par}}$ give the highest efficiency. This will be treated in the circuit design.

### IV. CIRCUIT DESIGN

#### A. Discrete component realization

To investigate the effect of the high frequency stimulation on the tissue a discrete component prototype of a buck-boost converter circuit was made (see Figure 4a). The goal was only to verify the functionality and no attention was paid to (power) efficiency.

The switching frequency on the PCB was also set to $2\,\text{MHz}$. The stimulator was connected to electrodes (percutaneous leads from St. Jude Medical) which were inserted into the mouth of a volunteer. The resulting electrode potential was measured and is depicted in Figure 4b.

The measured waveform has a bigger ripple than the results from Figure 3. This can be explained by the dispersion of the tissue. To reduce the ripple it was decided to increase the switching frequency to $10\,\text{MHz}$. This was not possible with the PCB, but this will be implemented in the eventual IC.

Most important result of the measurements is that the sense of stimulation was established for the volunteer: this means that stimulation is possible at such high frequencies.
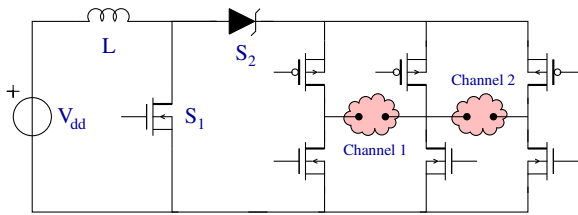
Fig. 5.  Implementation of a two channel Boost stimulator



Fig. 6.  Postlayout simulations of the circuit of Figure 5

## B. IC design

Based on the discussion above two circuits were designed to prove the operating principle of this system: one boost converter and one buck-boost converter. Here the design of the boost converter will be treated shortly. The circuit principle is depicted in Figure 5. The technology used is AMS $0.18\mu$m High Voltage technology.

As can be seen the circuit has two channels and it allows for stimulating one of the two channels or both simultaneously. Furthermore switch $S_2$ has been implemented using a Schottky diode to keep the control of the circuit easy. The size of the transistors was chosen such that the parasitic capacitances were kept to a minimum, while the resistive losses were still acceptable: the width is $100\,\mu$m for $S_1$ (with minimum length $400\,$nm) and $150\,\mu$m for the other switches.

The gates of the transistors are controlled using logic that controls the active channel(s) and the direction of stimulation. The gates of the PMOS transistors are controlled using a standard level shifter that shifts the voltage up to $10\,$V. This voltage is supplied from an external supply. Since the energy associated with switching is small, this can be generated on chip with a charge pump in future designs.

Figure 6 shows the post-layout simulation results of the circuit for simultaneous stimulation of both channels (both channels use the same intensity now). To model the bondwire and PCB capacitance of the inductor terminal, a $1\,$pF capacitor was added at the output of the bondpad. Using this circuit an efficiency of approximately 60% was achieved for $\delta$ ranging from 0.05 up to 0.3, corresponding to an output voltage range of approximately $4\,$V up to $10\,$V.

Compared with an ideal linear current source, which has an efficiency of $V_{\mathrm{stim}}/V_{\mathrm{dd}}$, the proposed stimulator will have a better power efficiency for low output values. Current sources operating in class G or H (addaptive supply voltage) are hard to compare: the efficiency highly depends on the implementation of the class G/H operation and may also depend on the output levels and tissue impedance values. Compared to these circuits the proposed circuit uses a minimum number of external components.

In the future a more sophisticated version of the system will be developed. The circuit currently lacks feedback control for the output voltage or current. Furthermore the inductor current will start to ring when the Schottky diode becomes reverse biased. Also, when the system is designed to work with bigger electrodes (yielding a higher output current), the capacitive losses decrease. The efficiency can then be as high as 80% over the full output range.
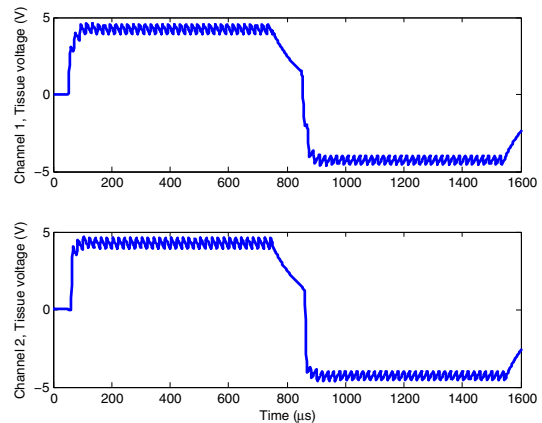
## V. CONCLUSION

A novel system design for neurostimulator circuits is proposed. It combines the voltage converter and stimulator output stage in a single system block and uses switched-mode stimulation for high energy efficiency. Furthermore the number of external components is reduced significantly by using the capacitance of the tissue as a filter.

The system operates at a high switching frequency of $10\,$MHz. It was verified with a descrete component realization that such stimulation can be effective. Furthermore an Integrated Circuit solution has been presented with two independent stimulation channels which only uses one inductor as an external component.

## REFERENCES

[1] S. Arfin and R. Sarpeshkar, "An energy-efficient, adiabatic electrode stimulator with inductive energy recycling and feedback current regulation," *IEEE Transactions on Biomedical Circuits and Systems*, vol. 6, pp. 1–14, 2012.

[2] K. Sooksood, E. Noorsal, J. Becker, and M. Ortmanns, "A neural stimulator front-end with arbitrary pulse shape, hv compliance and adaptive supply requiring 0.05mm2 in 0.35m hvcmos," in *IEEE International Solid-State Circuits Conference (ISSCC) Digest of Technical Papers*. IEEE, February 2011, pp. 306–308.

[3] S. Kelly and J. Wyatt, "A power-efficient neural tissue stimulator with energy recovery," *IEEE Transactions on Biomedical Circuits and Systems*, vol. 5, no. 1, pp. 20–29, February 2011.

[4] C. Butson and C. McIntyre, "Tissue and electrode capacitance reduce neural activation volumes during deep brain stimulation," *Clinical Neurophysiology*, vol. 116, pp. 2490–2500, 2005.

[5] S. Gabriel, R. Lau, and C. Gabriel, "The dielectric properties of biological tissues iii: Parametric models for the dielectric spectrum of tissues," *Physics in Medicine and Biology*, vol. 41, no. 11, pp. 2271–2293, November 1996.

[6] M. Ortmanns, A. Rocke, M. Gehrke, and H. Tiedtke, "A 232-channel epiretinal stimulator asic," *IEEE J. Solid-State Circuits*, vol. 42, pp. 2946–2959, 2007.

[7] K. Sooksood, T. Stieglitz, and M. Ortmanns, "An active approach for charge balancing in functional electrical stimulation," in *IEEE ISCAS*, May 2009, pp. 341–344.

[8] M. Schuettler, M. Franke, T. Krueger, and T. Stieglitz, "A voltage-controlled current source with regulated electrode bias-voltage for safe neural stimulation," *Journal Neuroscience Methods*, vol. 171, pp. 248–252, 2008.